



## Molecular Crystals and Liquid Crystals Science and Technology. Section A. Molecular Crystals and Liquid Crystals

Publication details, including instructions for authors and subscription information:

<http://www.tandfonline.com/loi/gmcl19>

## Smectic Polymorphism and Fluctuations in a Polar Liquid-Crystal Binary Mixture

Y. Shi<sup>a</sup>, G. Nounesis<sup>b</sup>, C. W. Garland<sup>c</sup> & Satyendra Kumara<sup>a</sup>

<sup>a</sup> Department of Physics, Kent State University, Kent, OH, 44242, USA

<sup>b</sup> Institute of Radioisotopes & Radiodiagnostic Products, National Center for Scientific Research "Demokritos", 153 10, Aghia Paraskevi, Greece

<sup>c</sup> Department of Chemistry, Massachusetts Institute of Technology, Cambridge, MA, 02139, USA

Version of record first published: 24 Sep 2006

To cite this article: Y. Shi, G. Nounesis, C. W. Garland & Satyendra Kumara (2000): Smectic Polymorphism and Fluctuations in a Polar Liquid-Crystal Binary Mixture, Molecular Crystals and Liquid Crystals Science and Technology. Section A. Molecular Crystals and Liquid Crystals, 351:1, 119-125

To link to this article: <http://dx.doi.org/10.1080/10587250008023260>

Full terms and conditions of use: <http://www.tandfonline.com/page/terms-and-conditions>

This article may be used for research, teaching, and private study purposes. Any substantial or systematic reproduction, redistribution, reselling, loan, sub-licensing, systematic supply, or distribution in any form to anyone is expressly forbidden.

The publisher does not give any warranty express or implied or make any representation that the contents will be complete or accurate or up to date. The accuracy of any instructions, formulae, and drug doses should be independently verified with primary sources. The publisher shall not be liable for any loss, actions, claims, proceedings, demand, or costs or damages whatsoever or howsoever caused arising directly or indirectly in connection with or arising out of the use of this material.

## Smectic Polymorphism and Fluctuations in a Polar Liquid-Crystal Binary Mixture

Y. SHI<sup>a</sup>, G. NOUNESIS<sup>b</sup>, C.W. GARLAND<sup>c</sup> and  
SATYENDRA KUMAR<sup>a</sup>

<sup>a</sup>*Department of Physics, Kent State University, Kent OH 44242, USA,* <sup>b</sup>*Institute of Radioisotopes & Radiodiagnostic Products, National Center for Scientific Research "Demokritos", 153 10 Aghia Paraskevi, Greece and* <sup>c</sup>*Department of Chemistry, Massachusetts Institute of Technology, Cambridge MA 02139, USA*

High-resolution x-ray diffraction studies have been performed on the polar liquid-crystal binary mixture of octyl- and decyl-oxyphenyl nitrobenzoyloxy benzoate (47.4 mole % DB<sub>8</sub>ONO<sub>2</sub> + 52.6 % DB<sub>10</sub>ONO<sub>2</sub>). At temperatures below 127 °C this mixture exhibits the phase sequence (with decreasing temperature) smectic-Ad – reentrant nematic N<sub>d</sub> – reentrant nematic N<sub>l</sub> – smectic-A<sub>1</sub> – tilted smectic antiphase smectic- $\tilde{C}$  – smectic-A<sub>2</sub> – smectic-C<sub>2</sub>. The development of lateral fluid antiphase fluctuations from the partial bilayer fluctuations in the smectic-A<sub>1</sub> phase have been probed and analyzed as well as the transition from the tilted smectic antiphase to the tilted bilayer smectic-C<sub>2</sub> phase that is accompanied by the occurrence of an intermediate smectic-A<sub>2</sub> phase.

**Keywords:** liquid-crystal phase transitions; calorimetry; x-ray scattering; tilted smectic antiphases

## INTRODUCTION

Smectic liquid crystals that are characterized by the competition of two incommensurate length scales, exhibit a rich variety of phases and phase transitions. For polar liquid-crystal systems the dipole-dipole molecular interactions result in the formation of antiferroelectric pairs of dimers with lengths  $l'$  that are temperature dependent and vary between  $l < l' < 2l$  where  $l$  is the molecular length. These length scales mark the monolayer, the partial bilayer and the bilayer smectic phases. The frustration caused by the competition between monolayer and partial bilayer ordering leads to reentrance phenomena of smectic and nematic phases as well as to the formation of smectic antiphases characterized by two-dimensional local order [1].

Theoretical phase diagrams demonstrating the existence of smectic antiphases were first proposed by Barois *et al* [2]. A fluctuation-corrected model by Prost and Toner [3] predicted phase diagrams exhibiting multiple reentrance of the nematic phase as well as of the partial bilayer smectic- $A_d$  phase. They also predicted the existence of a nematic - nematic critical point where the two nematic phases involved are characterized by short range monolayer and partial bilayer smectic order respectively.

Mixtures of the polar liquid crystals octyl- and decyl-oxyphenyl nitrobenzoyloxy benzoate ( $DB_8ONO_2$  and  $DB_{10}ONO_2$ ) are typical frustrated smectic systems and they have already been shown to exhibit most of the theoretically predicted characteristics [4]. At high temperatures and for mixtures  $\sim 50$  mole % in composition the following phase sequence has been observed: Isotropic (I) - Nematic (N) -  $Sm-A_d$  - Reentrant Nematic ( $N_r$ ) - Reentrant  $Sm-A_d$  -  $N_r$  - Monolayer Smectic- $A_1$  ( $Sm-A_1$ ) [5]. Detailed investigations of the very narrow concentration range  $51 < X < 54$  (where  $X$  is the mole % of  $DB_{10}ONO_2$  in the mixture) and in the vicinity of the end point of the first order  $Sm-A_d$  -  $Sm-A_1$  transition line and where the reentrant nematic phase is well established using AC calorimetry and high-resolution x-ray scattering revealed that a first order transition exists between two nematic phases  $N_d$  and  $N_1$ . These two nematic phases exhibited short range partial bilayer and monolayer smectic order respectively [6].

At lower temperatures a phase transition between the  $Sm-A_1$  phase and the tilted smectic antiphase  $Sm-\tilde{C}$  has also been studied [7]. In the present work the focus is in the phase transition  $Sm-\tilde{C} - Sm-C_2$

(tilted smectic bilayer phase). Previous calorimetric data have been analyzed using an "inverted" Landau model and based on the hypothesis that a Sm-A<sub>2</sub> (bilayer smectic) phase must occur at the Sm- $\tilde{C}$  - Sm-C<sub>2</sub> transition [5]. In the present work high-resolution x-ray scattering data demonstrate the existence of the Sm-A<sub>2</sub> phase in a very narrow temperature range intermediate between the Sm- $\tilde{C}$  and Sm-C<sub>2</sub> phases.

## RESULTS AND DISCUSSION

The high-resolution x-ray scattering studies have been conducted using a triple-axis four-circle diffractometer with a copper 15 kW rotating anode source and two germanium (111) single crystals that were used as monochromator and analyzer in a non-dispersive setup. The incident beam had a wavelength of 1.54178 Å and its size was adjusted to 1.5 mm horizontal and 6.0 mm vertical, by a pair of slits set at distance of 135 mm in front of the sample. The resolution of the diffractometer was  $\sim 4 \times 10^{-4} \text{ Å}^{-1}$  in the longitudinal direction,  $\sim 4 \times 10^{-5} \text{ Å}^{-1}$  in the transverse in-plane direction and  $2 \times 10^{-2} \text{ Å}^{-1}$  in direction perpendicular to the scattering plane. Two Na(Tl)I scintillation detectors were used to measure the intensity of the scattered and the incident beam. All the intensity measurements presented here are measured against a fixed number (10000) of counts of the incident beam in order to assure that power fluctuation will not affect the measurements.

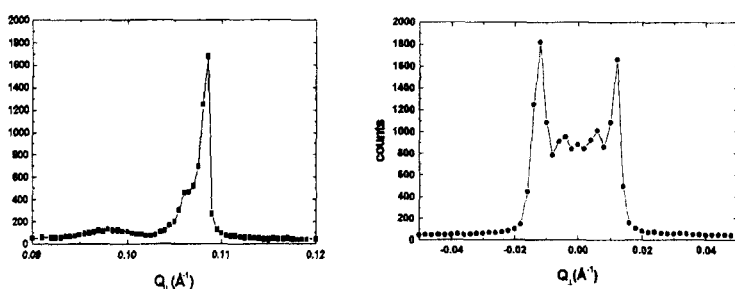


FIGURE 1 Longitudinal  $Q_{\parallel}$  scan at the wave vector  $q_2'$  and transverse  $Q_{\perp}$  scan for the off-axis peaks  $q_1'$  and  $q_2'$  at temperature  $T = 101.1 \text{ °C}$ , in the Sm- $\tilde{C}$  phase.

The growth of the smectic antiphase modulation in the Sm-A<sub>1</sub> phase can be illustrated via the development of the Sm-A<sub>d</sub> peak at  $q'$  (0, 0, 0.135) Å<sup>-1</sup>. At this wave vector, off-axis peaks begin developing upon cooling in the Sm-A<sub>1</sub> phase and when the Sm- $\tilde{C}$  phase is fully established just below the Sm-A<sub>1</sub> - Sm- $\tilde{C}$  phase transition, it is marked by two pairs of condensed off-axis Bragg peaks. The first pair is at  $q_1'$  (-0.012, 0, 0.1085) Å<sup>-1</sup> and  $(2q_0 - q_1')$  with  $2q_0$  at (-0.025, 0, 0.205) Å<sup>-1</sup> and the second pair at  $q_2'$  (0.012, 0, 0.1085) and  $(2q_0 - q_2')$  with  $2q_0$  at (0.025, 0, 0.205). Figure 1 shows longitudinal and transverse scans for  $q_1'$  and  $q_2'$  at 101.1 °C and some diffuse scattering centered at (0, 0, 0.098) Å<sup>-1</sup>.

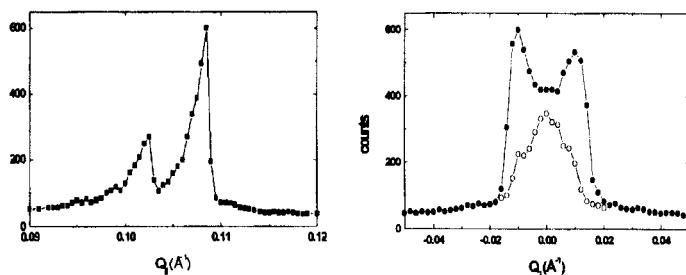


FIGURE 2 At temperature  $T = 101$  °C, in the Sm- $\tilde{C}$  phase, diffuse on-axis scattering at  $q_0$  associated with the Sm-A<sub>2</sub> phase appears while the two antiphase off-axis peaks at  $q_1'$  and  $q_2'$  move closer to each other.

At a lower temperature, 101 °C, diffuse on-axis scattering appears at (0, 0, 0.1025) Å<sup>-1</sup> commensurate with the  $2q_0$  peak, signaling the gradual development of the Sm-A<sub>2</sub> phase. On the other hand, as it can be seen in Figure 3 the  $q'$  off-axis peaks have moved closer to each other at a smaller wave vector ( $\pm 0.010$ , 0, 0.1083) Å<sup>-1</sup>. At 100.5 °C the system appears to be in a phase coexistence region, between the phases Sm- $\tilde{C}$  and Sm-A<sub>2</sub>. This is demonstrated by the data presented in Figure 3. At this temperature both the on-axis and off-axis peaks are condensed although the  $q_0$  peak located now at (0, 0, 0.1030) Å<sup>-1</sup> has gained in intensity over the  $q'$  peaks located at ( $\pm 0.008$ , 0, 0.1065) Å<sup>-1</sup>.

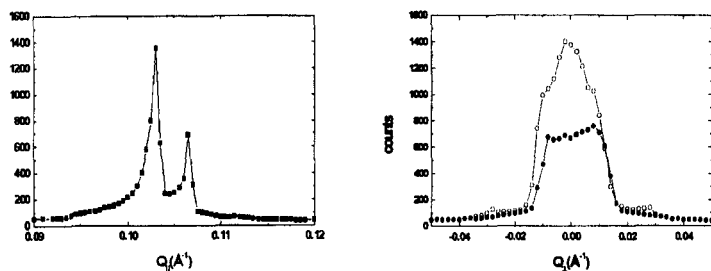


FIGURE 3 Longitudinal and transverse scans at temperature  $T = 100.5^\circ\text{C}$ , very near the  $\text{Sm-}\tilde{\text{C}} - \text{Sm-A}_2$  phase transition. The condensed on-axis scattering at  $q_0$  gains in intensity and coexists with the two antiphase off-axis peaks at  $q_1'$  and  $q_2'$ .

At  $100.3^\circ\text{C}$  the off-axis antiphase peaks have disappeared. Two on axis peaks are found at  $2q_0 = 0.209 \text{\AA}^{-1}$  and  $q_0 = 0.1045 \text{\AA}^{-1}$  with identical  $\omega$ -scans. This is the signature for the full establishment of the bilayer  $\text{Sm-A}_2$  phase (Figure 4). Molecular tilt begins to develop upon cooling right below this temperature signaling the onset of the  $\text{Sm-C}_2$  phase. The tilt reaches  $14^\circ$  at temperature  $T = 87.5^\circ\text{C}$  and the sample crystallizes at  $87.3^\circ\text{C}$ .

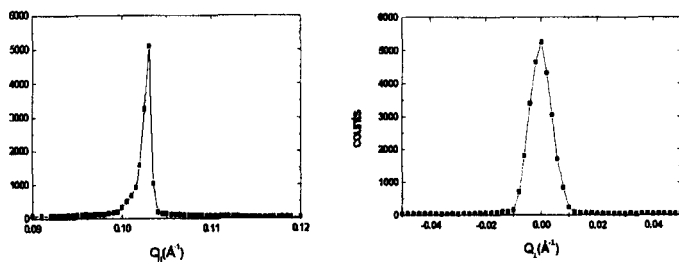


FIGURE 4 Longitudinal and transverse scans at temperature  $T = 100.3^\circ\text{C}$ . The single condensed on-axis scattering at  $q_0$  demonstrates the occurrence of the  $\text{Sm-A}_2$  phase.

It is remarkable that the high-resolution x-ray scattering technique has demonstrated the existence of the very narrow ranged but nevertheless thermodynamically stable Sm-A<sub>2</sub> phase. Previous calorimetric work investigating the same binary mixtures at concentrations in the vicinity of  $X = 52.7$  ( $X = 51.3$  and  $X = 55$ ) have found only one large heat capacity anomaly that had to be associated with the Sm- $\tilde{C}$  - SmC<sub>2</sub> phase transition [5]. Figure 5 displays the  $C_p$  data for the 51.33 mixture. As it can be seen the  $C_p$  peak is characterized by a long high temperature tail and by almost the complete absence of any excess heat capacity at the low temperature side.

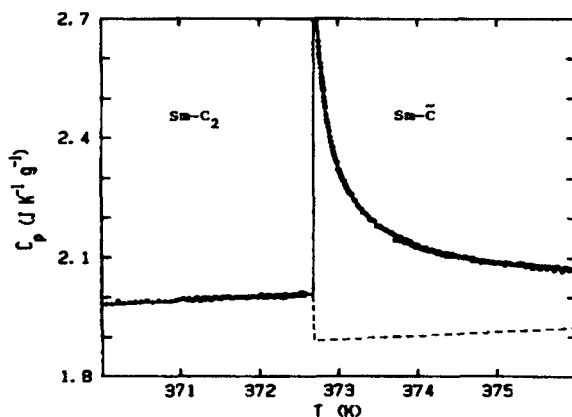


FIGURE 5  $C_p$  vs.  $T$  for the Sm- $\tilde{C}$  - SmC<sub>2</sub> phase transition. The straight line is the result of non-linear least-squares fit to the inverted Landau model. The dashed line shows the variation in the  $\Delta C_p$  term due to the possible Sm-A<sub>2</sub> - SmC<sub>2</sub> phase transition.

The  $C_p$  data presented in Figure 5 have been analyzed using an empirical inverted Landau model:

$$C_p = C_{p0} + \Delta C_p \quad \text{for } T < T_1 \quad (1a)$$

$$C_p = C_{p0} + A^* (T - T_k)^{-1/2} \quad \text{for } T > T_1 > T_k \quad (1b)$$



Here  $T_1$  is a first-order transition temperature, set within the range of the phase coexistence region. The quantity  $C_{p0}$  is the regular background contribution to the heat capacity given by  $B + E\Delta T$  where  $\Delta T = T - T_1$ . Non-linear least-squares fits of the data presented in Figure 5 with the "inverted" Landau equations 1a and 1b give very excellent results with the following values for the fitted parameters:  $T_1 = 372.669$  K,  $T_k = 372.629$  K,  $A^* = 0.265$  JK<sup>-1/2</sup>g<sup>-1</sup>,  $\Delta C_p = 0.119$  JK<sup>-1</sup>g<sup>-1</sup>,  $B = 1.890$  JK<sup>-1</sup>g<sup>-1</sup>,  $E = 9.96 \times 10^{-3}$  JK<sup>-2</sup>g<sup>-1</sup> and  $\chi_v^2 = 0.98$ .

It is important to note that in the derivation of equations 1a and 1b from the respective free-energy expressions, it was an absolutely necessary requirement to assume the occurrence of a narrow ranged Sm-A<sub>2</sub> phase intermediate between the Sm- $\tilde{C}$  and Sm-C<sub>2</sub> phases. While equation 1b describes the transition from Sm-C to Sm-A<sub>2</sub>, (the "inverted" Landau model actually describing the disappearance of the molecular tilt) the transition from Sm-A<sub>2</sub> to Sm-C<sub>2</sub> will justify the presence of the  $\Delta C_p$  term in equation 1a. Step-like behavior for this transition similar to the one proposed here has indeed been observed in other polymorphic smectic systems [8].

In summary, the high-resolution x-ray scattering measurements presented here, fully justify the use of the "inverted" Landau model for the description of the heat capacity behavior in systems exhibiting only one heat capacity anomaly for the phase sequence Sm- $\tilde{C}$  - Sm-A<sub>2</sub> - Sm-C<sub>2</sub>. The presence of the narrow ranged intermediate non-tilted smectic bilayer phase appears to be always required for the transition from the tilted smectic antiphase to the tilted smectic bilayer phase and this can only be understood as a necessary reorientation stage of the smectic layers.

## References

- [1] G. Sigaud, F. Hardouin and M.F. Achard, *Phys. Lett.*, **72A**, 24 (1979); A.M. Levelut, R.J. Tarento, F. Hardouin, M.F. Achard and G. Sigaud, *Phys. Rev. A*, **24**, 2180 (1981); C.R. Safinya, W.A. Varady, L.Y. Chiang and P.Dimon, *Phys. Rev. Lett.*, **57**, 432 (1986); E. Fontes, P.A. Heiney, J.L. Haseltine and A.B. Smith III, *J. Phys. (France)*, **47**, 1533 (1986).
- [2] P. Barois, J. Prost and T.C. Lubensky, *J. Phys. (France)*, **46**, 391 (1985).
- [3] J. Prost and J. Toner, *Phys. Rev. A*, **36**, 5008 (1987).
- [4] V.N. Raja, R. Shashidhar, B.R. Ratna, G. Heppke and Ch. Bahr, *Phys. Rev. A*, **37**, 303 (1989).
- [5] K. Ema, G. Nounesis, C.W. Garland and R. Shashidhar, *Phys. Rev. A*, **39**, 2599 (1989).
- [6] G. Nounesis, S. Kumar, S. Pfeiffer, R. Shashidhar and C.W. Garland, *Phys. Rev. Lett.*, **73**, 565 (1994).
- [7] Y. Shi, G. Nounesis and S. Kumar, *Phys. Rev. E*, **54**, 1570, (1996); Y. Shi, G. Nounesis, C.W. Garland and S. Kumar, *Phys. Rev. E*, **56**, 5575, (1997).
- [8] Y.H. Jeong, K.J. Stine and C.W. Garland, *Phys. Rev. A*, **37**, 3465 (1988).